26th INTERNATIONAL CONGRESS ON SOUND AND VIBRATION
7-11 July 2019, Montreal

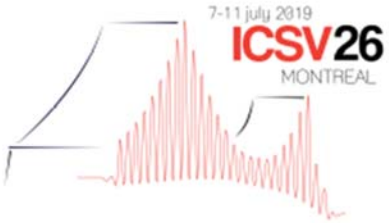

NUMERICAL STUDY OF A SWIRL ATOMIZED SPRAY RESPONSE TO ACOUSTIC PERTURBATIONS

Alireza Ghasemi, J.B.W. Kok
University of Twente, Enschede, The Netherlands
email: alireza.ghasemi@utwente.nl

A numerical study of the spray evaporation response to acoustic perturbations is presented. Thermoacoustic instabilities are the result of a resonant loop between the acoustic pressure waves in the form of velocity fluctuations and the heat release of the combustion phenomena. Premixed flame instability can be relatively simply characterized through the flame transfer function (FTF). In the case of non-premixed and partially premixed spray flames, the droplet atomization and subsequent evaporation is known to be related to the heat release rate of the combusting flame and have an effect on the resulting FTF. This paper examines the interaction between the acoustic field perturbation and the droplet evaporation by means of a numerical simulation of a pressurized Airblast type swirl atomizer. The fuel droplets are introduced into the computational domain of the burner at the location of film release and break up in a simplified droplet injection model. The resulting Eulerian-Lagrangian fuel spray simulation is used to represent the spray evolution after fuel film breakup within the shear region of the swirl atomizer. The droplet evolution is studied in the downstream region. In contrast with observations in other burners, in this specific burner design, the evaporation phenomena do not respond significantly to the high frequency velocity forcing. The interplay between the slip velocity perturbations and the vaporization rate is shown to have a complicated dependency on forcing amplitude in swirl atomizers.
Keywords: Turbulent combustion, Airblast Swirl Atomizer, Thermoacoustics, Evaporative Sprays

1. Introduction

The growing concern of global climate change has been the trend setter in many power generation and propulsion system designs and applications [1]. The need to bring down emission levels and moving towards cleaner combustion systems in aero engines has led to a shift away from the Rich-Burn, Quick-Mix, Lean-Burn (RQL) methods and towards lean premixed (LPM) combustion operation [2]. The lean operation mode has been a significant step towards clean combustion; however, lean combustion is shown to be more sensitive to Thermoacoustic instabilities. Turbulent flames normally exhibit heat release rate fluctuations that emit noise over a broad frequency range. In the case of operation under LPM, however, the unsteady nature of heat release of the flame as well as the flow perturbations in the combustor result in a resonant loop established between the flow, combustion and the acoustic modes of the system [3].

Thermoacoustic instabilities appear to be non-linear in nature and difficult to predict. They are an emergent instability of a complicated combustion system comprised of liquid fuel injection, atomization,

droplet vaporization and combustion [4][5]. Many studies on thermoacoustic instabilities focus on deriving the flame transfer function (FTF) and determine the unstable frequencies of the system through examining the effect of various forcing frequencies [6][7]. Atomization itself plays a crucial role and its interaction with the acoustic forcing is of great interest. In this work, we aim to study the effect of acoustic forcing on the vaporization rate of droplets in an isolated manner after the breakup process. The steady state flow within the studied swirl atomizer already shows fluctuations in velocity values. The effect of acoustic fluctuations on top of these variations in velocity is the aim of this study.

2. Methodology

Continuous operation of the studied Airblast swirl atomizer involves a complex chain of physical events including fuel injection, atomization, evaporation and combustion within the swirl atomizer. In this work, we explore the effect of acoustic forcing on the evaporation rate in isolation of the other phenomena. This is done in order to provide insight into the interplay of the acoustic perturbations on the evaporation rate of droplets of various size without the effect of primary and secondary breakup of the fuel.

With that goal in mind, and in order to minimize the breakup effects from the numerical study, droplets of a specific diameter are released into the flow field at a representative location. Droplet injection location is chosen downstream of the shear region of the flow where the fuel film is introduced into the Swirler. Injection is done through a ring with a thickness corresponding to the expected fuel film thickness within the Swirler with no cone angle. The droplets follow the flow field and evaporate along their pathway.

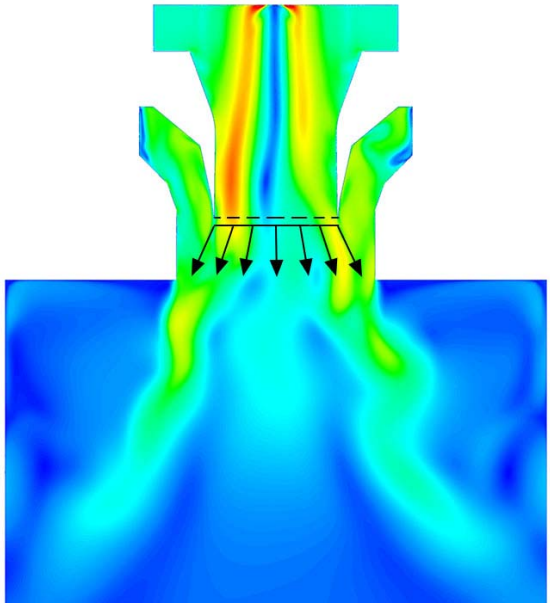

Figure 1: Scheme of Swirler with the indicated injection ring 2mm downstream of the shear zone

Acoustic forcing is implemented upstream of the shear location. This results in a sinusoidal shift in local flow velocities experienced at the location of each particle. Transient simulation is carried out to cover a number of acoustic periods corresponding to the forcing frequency of $2500\ Hz$ and for each defined droplet injection diameter. The results of the forced simulation is compared to an unforced evaporative spray simulation.

3. Numerical Setup

The numerical analysis is carried out using the commercial package, Ansys CFX v19.2. The non-symmetrical nature of the studied Airblast swirl atomizer calls for a fully 3D simulation of the flow. The geometry for the swirl atomizer is comprised of two distinct inlets for primary and secondary airflow through ducts. Each inlet is comprised of 8 ducts and the two flows meet downstream in a shear region where the fuel film is introduced into the domain. The fuel film is subsequently broken up into ligaments and eventually, form droplets which will disperse through the domain and evaporate. In the simulations considered here, fuel droplets are introduced in to the domain with a fixed diameter at a location downstream of the shear region representing the breakup distance.

The computational domain is comprised of around 20 million elements with element size in the shear region of the flow at $0.5\,mm$. Preliminary simulations determined the mesh quality and the proper boundary layer mesh sizing. Upon subsequent post processing of the RANS simulations, it was concluded that the ratio of airflow through primary and secondary inlets of the swirl atomizer can be used to truncate the computational domain. The corresponding flow velocities through each inlet was set on the inlet ducts alone, effectively allowing us to eliminate the upstream casing of the Swirler.

The URANS simulation is carried out in an Eulerian-Lagrangian manner where the fuel droplets are modelled by means of Lagrangian tracking and the gaseous phase is treated in an Eulerain manner as a continuous phase. The gaseous phase equations include the conservation equations for mass, momentum and energy equations. The species considered are Oxygen and Nitrogen mass fractions for air and n-Dodecane vapour phase mass fractions. The Lagrangian phase equations include conservation equations for mass, momentum and energy of the dispersed phase of fuel. The two sets of equations are coupled through the relevant source terms in each equation.

Shear stress transport model was selected as an adequate turbulence model for the Airblast swirl atomizer. This two-equation model uses one equation for the turbulence kinetic energy and one for the turbulent frequency. In order to ensure adequate treatment of near wall regions, a preliminary simulation was used to confirm suitable number of prism elements within the boundary layer.

The Particle Transport Fluid model was selected to model the Lagrangian phase droplets. The diameter is set to be a predefined fixed value without any variation or diameter distribution. The particle diameter is also linked to its equivalent mass and will shrink upon further vaporization of the droplet. Buoyancy effects are also considered given the nature of multiphase simulation. The Lagrangian phase is simulated in a fully coupled manner where the modified flow field in the presence of particles can affect the particle trajectories in return. Drag force exerted on each particle travelling through the domain is given by the following equation:

$$\vec{F}_D = 0.5 C_D \rho_g A_p |\vec{V}_{slip}| . \vec{V}_{slip} \quad (1)$$

Where $\vec{V}_{slip}$ is the relative velocity between each particle and its surrounding gas. ρ_g is the gaseous phase density and A_p is the projected particle area in the direction of movement. Slip velocity is the variable which undergoes cyclic oscillations in the acoustically forced simulation and is expected to have a significant impact on evaporation rate. Modified Schiller-Naumann [8] drag force model is considered to model the spherical particle drag coefficient, C_D, within the flow.

$$C_D = \max\left(\frac{24}{Re}(1 + 0.15Re^{0.687}), 0.44\right) \quad (2)$$

The Ranz-Marshall correlation [9] is used as the interphase heat transfer model. The correlation applies for flow past a spherical particle and relates the Sherwood number to Reynolds number and Prandtl number in this manner:

$$Sh = 2 + 0.6Re^{0.5}Pr^{0.3} \quad (3)$$

Sherwood number effectively defines the heat transfer rate for the droplets and it shows the effect of the Reynolds number on the evaporation rate. Light oil modification bases the parameters used in the calculation of Reynolds number, Nusselt number and Sherwood number on the gas in the boundary layer of the droplets which itself is governed by the Antoine equation in the following manner:

$$p_{sat} = p_{scale} \exp\left(A - \frac{B}{T + C}\right) \quad 4$$

A, B and C are the Antoine equation coefficients for n-Dodecane. p_{scale} is the modification that scales the units for the vapour pressure as described above. Particles experience evaporation through the following equation [10]:

$$\frac{dm_p}{dt} = \pi d_p \rho_l D_l Sh \frac{W_C}{W_g} \ln\left(\frac{1 - X_s^V}{1 - X_{vap}^V}\right) \quad 5$$

Where d_p is the diameter of each droplet, $\rho_l D_l$ is the dynamic diffusivity of the droplets within the gaseous phase and Sh is the Sherwood number. W_C and W_g are the molecular weight of the vapour and mixture in gaseous phase. X_s^V represents mole fraction of n-Dodecane at droplet surface and X_{vap}^V is the mole fraction of n-Dodecane in the gaseous phase.

The fuel considered in the corresponding experimental setup is kerosene. Following the standard convention, n-Dodecane was selected as a surrogate fuel with comparable properties. The Swirler is set to operate at an elevated pressure of 3 bar and a temperature of 573 K. This corresponds to an air mass flow rate of $0.1733\ kg/s$. Based on an energy balance for the whole combustor and in order to limit the flue gas temperature at the outlet, the fuel mass flow rate is set to $4.34\ g/s$. Droplets are injected at the saturation temperature of n-Dodecane at $3\ bar$.

Injection of droplets initiate from a ring cone zone with zero cone angle. This effectively represents the fuel film after complete atomization into fuel ligaments and subsequent droplets. The location of the injection ring, therefore, was selected to be $2mm$ downstream of the fuel film release to represent the total atomization distance needed for the formation of droplets. Thickness of the ring is defined using the flow field information as well as the known desired fuel mass flow rate. A preliminary simulation was used to determine a reasonable droplet velocity 2mm downstream of the fuel film and a thickness of around 4 microns was therefore selected for the ring thickness.

Acoustic forcing is implemented in the code in a way that the mass flow rate upstream at the inlets gets modulated by a certain amplitude around the mean value with the following equation:

$$u = \bar{u} + u' \quad 6$$
$$u' = A \sin(\omega_f t)$$

The modulation constant A is defined equal to 0.12 of the mean value. ω_f is chosen on the basis of the forcing frequency of $2500\ Hz$ .This results in a defined acoustic forcing period T_{ac} of about $0.04\ ms$. Relaxation time for the droplets is the other important time scale of this analysis provided by the following equation:

$$\tau_p = \frac{\rho_p\, d_p^2}{18\, \mu_g} \quad 7$$

Where ρ_p and d_p^2 are the droplet density and diameter, respectively. μ_g is the dynamic viscosity of the gaseous phase. Relaxation time, in this case, for particles of $20\ microns$ in size is about $0.6\ ms$ which corresponds to $1.6T_{ac}$. Transient simulations were carried out with a time step of $6.6\ \mu s$ and were continued until a steady state axial penetration length was achieved at $0.014\ s$ corresponding to $35T_{ac}$.

4. Results

Transient nature of the flow within the swirl atomizer results in a natural oscillation of velocity at a given location. Still, the acoustic forcing results in a velocity oscillation on top of the transient velocities as evident in the following figure.

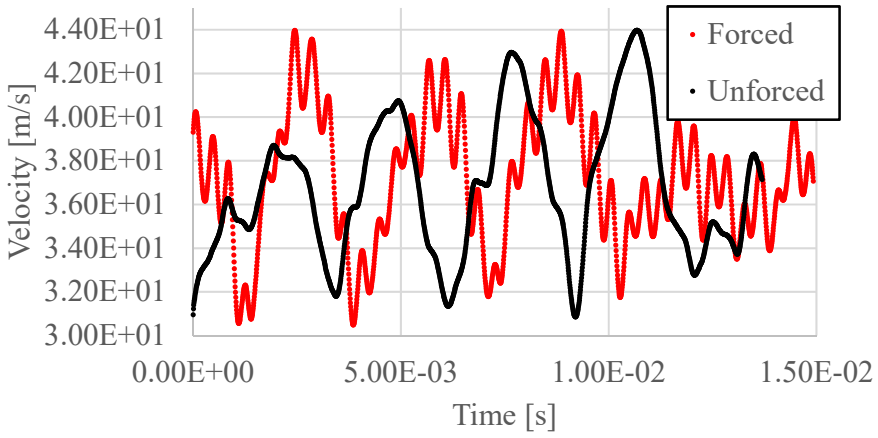

Figure 2: Velocity magnitude at a representative point in the two simulated cases

One important aspect of the droplet injection is the axial and radial penetration values defined as the distance within which 99% of the droplet mass is located. Axial penetration in the steady case reaches 21.9 cm in the Unforced simulation and slightly lower in the Forced case, at 20.1 cm. Acoustic forcing seems to have reduced the axial penetration value but the effect is not significant.

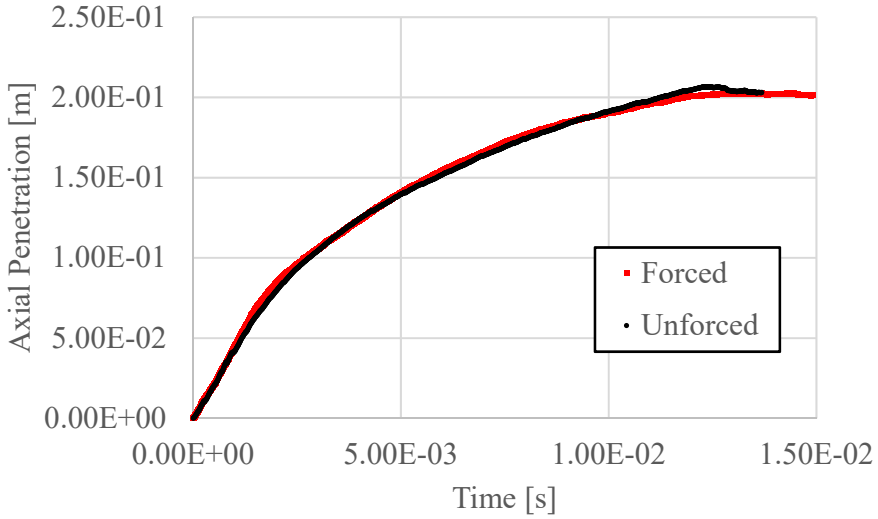

Figure 3: Axial and Radial penetration for both studied cases

Looking into 100 randomly selected pathways for droplets of each size, droplet size variation along their trajectories can be visualized. At the droplet release location, droplet sizes are fixed to the predefined value. As the droplets travel through the domain, due to evaporation and the mass exchange with the gaseous phase, they shrink in size. It is noteworthy that the bigger droplets tend to be resilient to the

fluctuations of velocity and smaller droplets get entrained in the flow easier. This is confirmed in the results as the smaller droplets undergo higher acceleration upon being introduced to the domain.

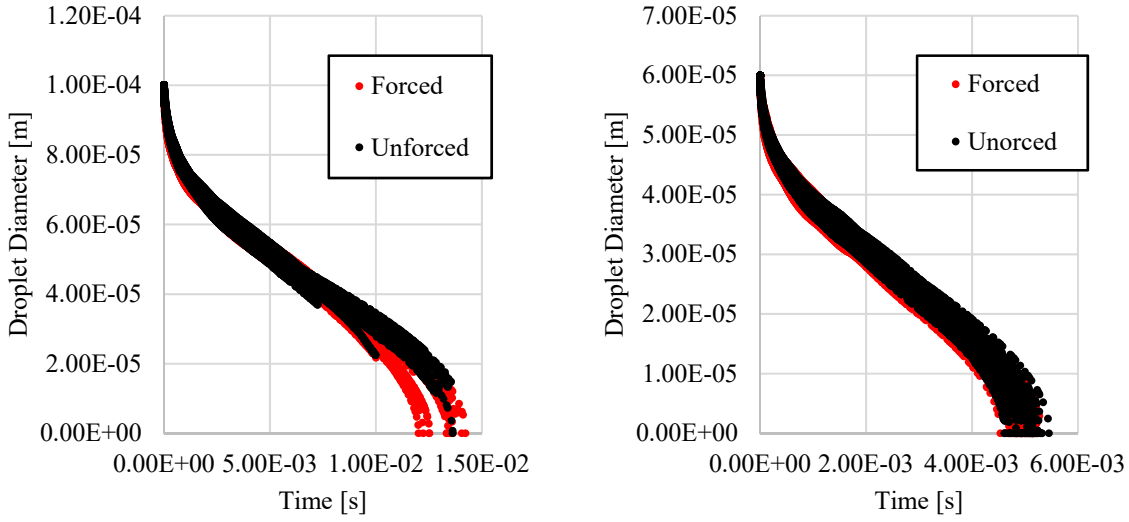

Figure 4: Droplet evaporation in time for droplet size of 100 micron (left) and 60 micron (right)

Larger droplets of 100 microns and 60 microns in size show little variation in presence of acoustic forcing. This could be due to the natural oscillations of the flow being the dominant where the larger droplets are found.

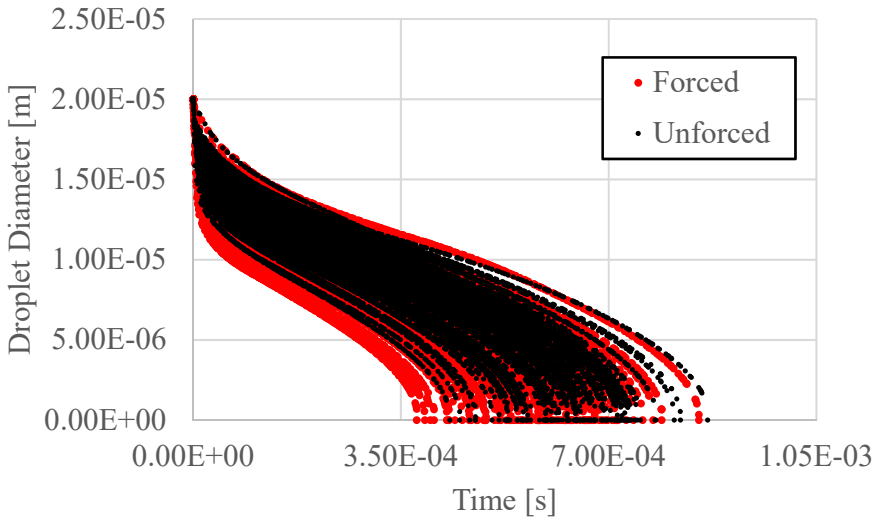

Figure 5: Droplet evaporation in time for droplets size of 20 micron

Smaller droplets show a wider deviation in diameter when the flow is forced. But even for these smaller droplets this effect is not pronounced. Visualization of slip velocities also confirmed that the acoustic forcing did not significantly enhance the slip velocities experienced by droplets of studied diameters. Slip Velocities are observed to reduce significantly as the droplets get entrained in the flow prior to full evaporation and show wider variation in the presence of acoustic forcing. Still, this effect is not strong enough to modify evaporation rates.

5. Conclusions

Evaporation of droplets under acoustic forcing within an industrial Airblast swirl atomizer has been studied. Forcing was applied at the two distinct inlet ducts of the Swirler. Droplets of three distinct diameters were released at a location downstream of the shear zone of the atomizer and the evaporation rate of the droplets was studied. The expected results are an enhanced evaporation rate for the droplets of larger diameter since they will not be able to follow the gas velocity and therefore, undergo a slip velocity oscillation. Smaller droplets tend to follow the streamlines easier due to their lower inertia and the resulting lower slip velocity could extend their lifetime within the flow. Acoustic forcing amplitude applied was 0.12 of the mean value. The obtained simulation results, however, reveal that the slip velocity experience by the droplets is only marginally changed due to acoustic forcing and the transient flow effects within the Swirler and the high velocities within the gaseous phase is dominating the acoustic effects. Acoustic forcing at the studied amplitude seems to have a more pronounced impact on smaller droplets. These effects, might still be significant in the presence of the flame where the acceleration of the flow post combustion will dramatically change the flow field and the heat release will modify the evaporation rates and they will be examined in a subsequent study.

6. Acknowledgements

This project has received funding from the European Union's Horizon 2020 research and innovation programme under the Marie Skłodowska-Curie grant agreement No. 766264.

REFERENCES

[1] IPCC, 2018: *Global warming of 1.5°C. An IPCC Special Report on the impacts of global warming of 1.5°C above pre-industrial levels and related global greenhouse gas emission pathways, in the context of strengthening the global response to the threat of climate change, sustainable development, and efforts to eradicate poverty* [V. Masson-Delmotte, P. Zhai, H. O. Pörtner, D. Roberts, J. Skea, P.R. Shukla, A. Pirani, W. Moufouma-Okia, C. Péan, R. Pidcock, S. Connors, J. B. R. Matthews, Y. Chen, X. Zhou, M. I. Gomis, E. Lonnoy, T. Maycock, M. Tignor, T. Waterfield (eds.)]. In Press.

[2] Y. Huang and V. Yang, "Dynamics and stability of lean-premixed swirl-stabilized combustion," *Prog. Energy Combust. Sci.*, vol. 35, no. 4, pp. 293–364, 2009.

[3] T. C. Lieuwen, *Unsteady combustor physics*. Cambridge University Press, 2012.

[4] V. Fratalocchi and J. B. W. Kok, "Modelling of the Dynamic Interaction Be- Tween a Reacting Spray and an Acoustic Field in a Turbulent Combustor," no. July, pp. 13–17, 2014.

[5] P. Gruhlke, I. Mahiques, J. Meisl, P. Kaufmann, A. Kempf, and J. B. W. Kok, "The Acoustic Response Of Reacting Sprays In Cross Flow Models To Forced Excitations."

[6] X. Han and A. S. Morgans, "Simulation of the flame describing function of a turbulent premixed flame using an open-source LES solver," *Combust. Flame*, vol. 162, no. 5, pp. 1778–1792, 2015.

[7] J. Su, A. Barker, A. Garmory, and J. Carrotte, "Spray Response to Acoustic Forcing of a Multi-Passage Lean-Burn Aero-Engine Fuel Injector," in *Volume 4A: Combustion, Fuels, and Emissions*, 2018, p. V04AT04A040.

[8] A. Schiller, L. and Naumann, "VDI Zeits, 77, p. 318," 1933.

[9] W. E. Ranz and J. W. R. Marshall, "Vaporation from Drops, Part I". Chem. Eng. Prog. 48(3). 141–146."

[10] "Ansys CFX-Solver Modeling Guide, Version 19.2."